Simulation analysis of mass and heat transfer attributes in nanoparticle flow subject to Darcy-Forchheimer medium

M. Imran Shahid[a,b], S. Ahmad[a], and M. Ashraf [a,*]

a. *Centre for Advanced Studies in Pure and Applied Mathematics, Bahauddin Zakariya University, Multan 60800, Pakistan.*
b. *Department of Mathematics, Government College of Science, Multan 60000, Pakistan.*

Abstract. This study develops a model to analyze the effect of chemical reaction in a Darcy-Forchheimer nanofluid mass and heat transfer flow over a nonlinearly extending surface with the effect of non-uniform magnetic force. Further, it is presumed that the fluid is viscous and incompressible. A powerful tool of similarity variables is exploited to transform the governing flow model PDEs into ordinary ones, which are then solved with the aid of the Successive Over Relaxation (SOR) technique using MATLAB software. Our outcomes are linked to those presented in the earlier research works in the literature and found to be in good agreement with them. The effects of different involved parameters are examined and visualized through tables and diagrams. From the current investigation, it is revealed that the chemical reaction enhances the mass transfer rate, whereas the Forchheimer parameter tends to devaluate the mass and heat transport rate on the surface. The magnetic and porosity parameters tend to increase the skin friction. The present results can be applied with caution to thermal control systems.

1. Introduction

In recent years, heat and mass transfer flows involving chemical reaction have several industrial and engineering applications, e.g., cooling methods for metal surfaces, nuclear power plants, chemical catalyst and processes, burning and boiler design, aerodynamic extrusion of synthetic sheets, engine oil, ethylene glycol, filtration, refrigeration, dispersal of medication in blood layers, etc. Kandasamy et al. [1] analyzed

the chemical reaction with Soret-Dufour existing on a convective spongy stretching surface. Gangadhar and Bhaskar [2] studied the Magneto-Hydrodynamic (MHD) mass and heat transport flow with the effect of chemical reaction through a porous channel having moving plates. Makinde et al. [3] described the effect of buoyancy strength and movement of thermal and magnetic forces over a stagnation point nanofluid flow along with stretching/shrinking sheet. A three-dimensional axisymmetric fluid flow was examined numerically by Turkyilmazoglu [4] using the perturbation approach.

The term nanofluid refers to a liquid that contains suspended tiny particles of diameter less than 100 nm. Nanoparticles are elemental to the investigation of blood flow, kidney transplant, hyperthermia, etc. Initially, Choi and Eastman [5] predicted that the spread of nanoparticles in base fluids generated the

---

*. *Corresponding author.*
 E-mail addresses: mishahidbzu@gmail.com (M. Imran Shahid); sohailkhan1058@gmail.com (S. Ahmad); muhammadashraf@bzu.edu.pk (M. Ashraf)

nanofluid which increased the thermal conductivity of the fluid. Later on, Masuda et al. [6] presented the properties of nanofluids. A numerical model of nanofluid, which displayed the distinctiveness of Brownian and thermophoresis movement of fluid, was premeditated by Buongiorno [7]. Khan and Pop [8] surveyed the thickness of boundary layer flow of nanofluid on a stretching sheet. The flow and heat transfer of the nanoliquid film flow over a moving inclined substrate was analyzed by Turkyilmazoglu [9]. The motion of nanoparticles was induced through both the gravitational force as well as the substrate movement. It was noticed that the film thickness was much reduced and the wall shear was amplified considerably in the presence of silver nanoparticles. Feizabad et al. [10] prepared the carbon nanotubes (CNTs) through mechanical milling of Hexane in the presence of two different catalysts, namely amorphous and crystalline. Thermal analysis was presented to characterize the CNTs. The results illustrate that the amorphous catalyst induces more structural defects in CNTs with respect to the crystalline catalyst. Jabeen et al. [11] concentrated on the characterization of Walters-B nanofluid flow to investigate the mechanism of irreversibility. Energy equation included radiation effects and heat generation phenomenon. Homotopy Analysis Method (HAM) was used to numerically solve the system of equations. Characterization and modeling of nanofluids were deliberated by Hakeem et al. [12] to improve the effects of heat transfer. Nanoparticles are much more helpful in biomedicine, military systems, electronics, supercomputers, nuclear reactors, etc. Further details can be seen in [13–18].

The MHD effect as taken in the concerned problem is of significance in such fields as geothermal structure, land water pollution, crude oil refinement, heat swap, electromagnetic pumps, storage of nuclear waste, blood flow measurements, and many more. Many researchers have investigated the effect of MHD in various fluid problems. Sharma and Singh [19] conducted the thermal conductivity analysis of MHD stagnation point Newtonian flow. Aziz and Khan [20] analyzed entropy generation in MHD flow with temperature-dependent thermal conductivity. Pal et al. [21] investigated the Soret and Dufour impacts on MHD convection through a porous medium using the power-law model. Hakeem et al. [22] discussed the MHD on stagnation point movement of nanofluid over a stretching/shrinking surface with critical and statistical methods. Turkyilmazoglu [23] focused on the MHD slip flow of an electrically conducting, viscoelastic fluid past a stretching surface. The main concern was to analytically investigate the structure of the solutions and determine the thresholds beyond which multiple solutions exist.

The movement of nanofluid through porous media is quite important, e.g., fermentation procedure of groundwater flow through rocks and mud, flow of blood through the tissues of the body, injection utilized for medical treatment, transport in drying process of wood, food products, soil mechanics, and so forth. Henry Darcy [24] reported the first contribution to the fluid dynamics considering the porosity factor. The outcomes were based on experimental and simulation analyses of a laminar and steady flow and these results were further analyzed by various researchers [25,26]. Darcy's law may not be quite applicable to some situations where the rate of the influence of fluid and motion is very high. The Darcy-Forchheimer flow of several fluids has been examined extensively. Transportation of nanomaterial within a tube was investigated numerically by Sheikholeslami et al. [27]. They employed Helical Tape (HT) with different width ratios to augment flow blockage. Multiple tapes caused resistance in the flow. Hayat et al. [28] solved a mathematical system for Darcy-Forchheimer flow by taking CNTs as nanoparticles. They employed the optimal HAM to find the approximate solution of their problem. In their analysis, the Nusselt number and the surface drag were noticed for both MWCNTs (Multiple-Walled Carbon Nanotubes) and SWCNT (Single-Walled Carbon Nanotubes).

The exact analytic solutions were employed to numerically analyze the heat transfer enhancement and efficiency of longitudinal rectangular fin profiles in case a stretching or shrinking mechanism was mounted on the surface of the fin [29]. A rigorous mathematical approach was presented by Turkyilmazoglu [30] to understand the transparent impacts of Buongiorno nanofluid model on the rate of heat and mass transfer in different fluid flow geometries. A novel technique called SOR method was used by Ali et al. [31] to determine the approximation solution of the hybrid nanoparticle flow with allowance for heat generation. The numerical representations and graphical illustrations were employed to elaborate the numerical outcomes. Sheikholeslami et al. [32] presented numerical and empirical analyses of thermal performance development in Flat Plate Solar Collectors (FPSCs). In this analysis, an updated review was carried out using nanofluids in FPSCs and photo voltaic therma (PVT) systems. The productivity of photovoltaic (PV) modules was reduced with an increase in the working temperature.

Caucao et al. [33] found the numerical solution of a nonlinear model that involved the Navier-Stokes and Darcy-Forchheimer equations with the Beavers-Joseph-Saffman condition on the interface. A study involving two-dimensional nanofluid flow in the presence of Ohmic dissipations, Darcy-Forchheimer medium, and second-order slip was carried out by Ganesh et al. [34]. The fourth-order RK method and shooting methodology were employed to obtain dual solutions.

Ullah et al. [35] numerically analyzed the 3D Darcy-Forchheimer flow of nanoliquids and stated that large estimates of thermophoresis force caused a substantial increase in the concentration and temperature distributions. The three-dimensional micropolar nanofluid flow between horizontal and parallel plates was examined by Khan et al. [36]. Their flow model equations involved the Darcy-Forchheimer term. Their results depicted that porous media affected the fluid motion upon reducing the velocity. Du et al. [37] developed a numerical technique to solve the nonlinear coupled Navier-Stokes/Darcy models. In this study, numerical and theoretical analyses were employed to interpret the significance of the numerical scheme (two-grid method). The stagnation-point mixed convective flow of cross liquid moving over a vertical plate entrenched in a Darcy-Forchheimer porous medium was probed by Khan et al. [38]. Buongiorno's model was considered in order to formulate a mathematical model, which described the MHD flow of a micropolar nanofluid over an exponential sheet in an Extended-Darcy-Forchheimer porous medium (see Lund et al. [39]). Rasool et al. [40] inspected the entropy optimization as well as heat and mass transport in Darcy-Forchheimer nanofluid flow surrounded by a non-linear stretching surface. Navier-Stokes model-based governing equations for non-Newtonian nanofluids having symmetric components in different terms were considered. Lund et al. [41] determined dual solutions in the specific range of shrinking/stretching parameters using shooting technique. Brownian and thermophoresis effects were also taken into account in this micropolar nanofluid flow.

Even though much relevant work exists in the available literature, the incompressible and electrically conducting flow of Darcy-Forchheimer nanofluid over a nonlinear stretching surface has not been explored numerically considering the role of chemical reaction (specifically). Therefore, the mathematical solutions of the concerned problem are achieved using the Successive Over Relaxation (SOR) technique. The behavior of preeminent parameters is presented in graphical and tabular forms. Some new results of recent research describing the characteristics of Darcy-Forchheimer porous medium in the flow involving the combined effects of magnetohydrodynamics and chemical reaction are developed.

2. Mathematical model

Consider a viscous and incompressible flow including MHD Darcy-Forchheimer nanofluid over a nonlinearly expanding surface. The electrical conductivity is increased by applying the varying magnetic field. The present model is specified by considering almost negligible magnetic Reynolds effect in the flow. The nonlinear sheet is placed alongside the x-direction and the y-axis
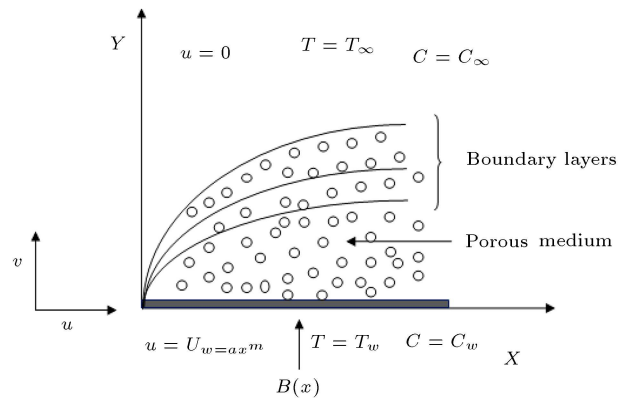

Figure 1. Physical model of the problem.

is considered at the right angle to the sheet. The sheet changes its position with stretchable velocity $U_w = ax^m$ along the positive x-direction, where $m > 0$ exhibits the nonlinear stretchable sheet. The fluid is electrically conducted due to the magnetic field effect. The Brownian diffusion along with thermophoresis is also assumed in the flow. A physical model is provided in Figure 1.

Under the above assumptions, the dominant flow model equations may be given as [42]:

$$\frac{\partial u}{\partial x} + \frac{\partial v}{\partial y} = 0, \tag{1}$$

$$v\frac{\partial u}{\partial y} + u\frac{\partial u}{\partial x} = v\frac{\partial^2 u}{\partial y^2} - \frac{\sigma B^2 x^{m-1}}{\rho}u - \frac{v}{k}u - \frac{C_b}{\sqrt{k}}u^2, \tag{2}$$

$$\frac{\partial T}{\partial y} + u\frac{\partial T}{\partial x} = \alpha\frac{\partial^2 T}{\partial y^2} + \frac{(\rho c)_{np}}{(\rho c)_{fn}}$$

$$\times \left[D_{Br}\frac{\partial T}{\partial y}\frac{\partial C}{\partial y} + \frac{D_{th}}{T_\infty}\left(\frac{\partial T}{\partial y}\right)^2 \right], \tag{3}$$

$$v\frac{\partial C}{\partial y} + u\frac{\partial C}{\partial x} = \frac{D_{th}}{T_\infty}\left(\frac{\partial^2 T}{\partial y^2}\right) + D_{Br}\left(\frac{\partial^2 C}{\partial y^2}\right)$$

$$- K\left(C - C_\infty\right). \tag{4}$$

The chemical reaction and magnetohydrodynamic terms have been taken into account in our model equations, which were not considered in [42]. The importance of the novel terms is associated with heat transportation and fluid past through a Darcy-Forchheimer porous (permeable) medium under the chemical reaction effect, and its importance and pertinence can be found in a large spectrum of technological, biological, biotechnological, and engineering mechanisms such as ground stream hydrology, drainage problems, chemical engineering, solar absorption and filtration, irrigation, hydrology, solar panels, solar cells, and so on. The relevant Boundary Conditions (BCs) are:

$$u = U_w = ax^m, \quad v = 0, \quad T = T_w, \quad C = C_w,$$

$$\text{at} \qquad y = 0, \tag{5}$$

$$u = 0, \qquad T = T_\infty, \qquad C = C_\infty,$$

$$\text{at} \qquad y \to \infty, \tag{6}$$

Define:

$$\left\{ u = ax^m \frac{\partial f}{\partial \eta}, \qquad v = -\left(\frac{1}{2}\sqrt{2av(n+1)x^{\frac{m-1}{2}}} \right) \right.$$

$$\left(f(\eta) + \left(\frac{m-1}{m+1} \right) \eta \frac{\partial f}{\partial \eta} \right), \qquad \theta(\eta) = \frac{T - T_\infty}{T_w - T_\infty},$$

$$\left. \phi(\eta) = \frac{C - C_\infty}{C_w - C_\infty}, \quad \eta = \frac{1}{2}\sqrt{\frac{2\rho_{fl}a(m+1)}{\mu}x^{\frac{m-1}{2}}y} \right\}. \tag{7}$$

Eqs. (1)–(6) in the light of Relation (7) take the following form:

$$\frac{\partial^3 f}{\partial \eta^3} + f\left(\frac{\partial^2 f}{\partial \eta^2} \right) - \left(\frac{2m}{m+1} \right) \left(\frac{\partial f}{\partial \eta} \right)^2$$

$$- M^2 \frac{\partial f}{\partial \eta} + Po \frac{\partial f}{\partial \eta} - Fr \left(\frac{\partial f}{\partial \eta} \right)^2 = 0, \tag{8}$$

$$\frac{\partial^2 \theta}{\partial \eta^2} + Pr \left(Nb \frac{\partial \theta}{\partial \eta} \frac{\partial \phi}{\partial \eta} + f \frac{\partial \theta}{\partial \eta} + Nt \left(\frac{\partial \theta}{\partial \eta} \right)^2 \right) = 0, \tag{9}$$

$$\frac{\partial^2 \phi}{\partial \eta^2} + Scf \frac{\partial \phi}{\partial \eta} + \frac{Nt}{Nb} \frac{\partial^2 \theta}{\partial \eta^2} - \frac{Kc}{m+1} Sc\phi = 0, \tag{10}$$

$$\left\{ f(0) = 0, \quad \theta(0) = 1, \quad \phi(0) = 1, \quad f'(0) = 1, \right.$$

$$\left. \theta(\infty) = 0, \quad \phi(\infty) = 0, \quad f'(\infty) = 0 \right\}, \tag{11}$$

where Po is porosity, M Magnetic number, Pr Prandtl number, Fr Forchheimer number, Nb Brownian parameter, Kc chemical reaction parameter, Sc Schmidt number, and Nt thermophoretic parameter. These parameters can be formulated as follows:

$$\left\{ M^2 = \frac{2\sigma B^2}{a\rho_f(n+1)}, \qquad Po = \frac{2v}{ka(m+1)x^{m-1}}, \right.$$

$$Fr = \frac{2C_{bx}}{k^{\frac{1}{2}(m+1)}}, \qquad Pr = \frac{v}{\alpha},$$

$$Nb = \frac{\rho c_{np} D_{Br}(C_w - C_\infty)}{(\rho c)_{fl}}, \qquad Kc = \frac{2K}{ax^{m-1}},$$

$$Sc = \frac{v}{D_{Br}}, \qquad Nt = \frac{\rho c_{np} D_{th}(T_w - T_\infty)}{v(\rho c)_{fl} T_\infty},$$

$$\left. \alpha = \frac{k}{\rho C_p} \right\}. \tag{12}$$

3. Methodology

It is difficult to seek an analytical solution to Eqs. (8)–(10) because of the involvement of coupled and highly nonlinear equations. Finding the analytical solution of the concerned problem can be extremely time-consuming, given that the model equations are 3rd-order differential equations. This is the reason why this study adopted numerical method instead of analytical method to solve the nonlinear Eqs. (8)–(10). Multiple solutions of a linear programming problem are solutions, each of which maximizes or minimizes the objective function. Multiple solutions can be used where both the objective function and one of constraint lines have the same slope. The multiple solutions can also be used in our problem only if we separately solve the governing equations, e.g., momentum, heat, and mass equations. To seek a numerical approximation to solve this system of equations under the BCs (11), the following criteria are adopted. Substituting $p = f'$ into Eq. (8), we obtain:

$$p = f' = \frac{df}{d\eta}, \tag{13}$$

$$p'' + fq' - \left(\frac{2m}{m+1} \right) q^2 - M^2 q - Poq - Frq^2 = 0, \tag{14}$$

$$\theta'' + Pr \left(Nb\theta'\phi' + f\theta' + Nt(\theta')^2 \right) = 0, \tag{15}$$

$$\phi'' + Scf\phi' + \frac{Nt}{Nb}\theta'' - \frac{Kc}{m+1}Sc\phi = 0, \tag{16}$$

with BCs:

$$\left\{ f(0) = 0, \quad \theta(0) = 1, \quad \phi(0) = 1, \quad f'(0) = 1, \right.$$

$$\left. \theta(\infty) = 0, \quad \phi(\infty) = 0, \quad f'(\infty) = 0 \right\}. \tag{17}$$

We initially discretize the domain $[0, \infty)$ with mesh size h_0 and then, integrate Eq. (13) by Simpson's rule [43]. Eqs. (14)–(16) are discretized at a typical lattice point $\eta = \eta_0$ at the interval $[0, \infty)$. The resulting equations are solved repetitively by the SOR method. The relaxation factor ω is chosen to be 1.65 for the fast convergence, because when we assign different values to ω, the number of iterations is reduced and the values of $f''(0) - \theta'(0)$, $-\phi'(0)$ are not changed (see

Table 1. Number of iterations when $m = 2.0$, $M = Nb = Po = Kc = 0.2$, $Fr = 0.1 = Nb$, $Sc = 1.0$ for different ω's.

ω	No. of iterations	$f''(0)$	$-\theta'(0)$	$-\phi'(0)$
0.3	49217	1.69881	0.39793	0.41798
0.6	22941	1.69881	0.39793	0.41798
0.9	13030	1.69881	0.39793	0.41798
1.2	7956	1.69881	0.39793	0.41798
1.5	4574	1.69881	0.39793	0.41798
1.8	1815	1.69881	0.39793	0.41798

Table 2. Comparison of $-\phi'(0)$ with that in the work of Rasool et al. [48] when $Kc = 0$.

Fr	Po	Present study	Rasool et al. [48]
0.0	1.0	0.4084	0.4085
0.6	–	0.3925	0.3925
1.2	–	0.3789	0.3789
0.2	0.0	0.4244	0.4244
–	0.5	0.3812	0.3812

Table 1). If the following criterion is fulfilled, the repetitive procedure is stopped.

$$\max\Bigg(\|f_{i+1} - f_i\|, \ \|q_{i+1} - q_i\|, \ \|\theta_{i+1} - \theta_i\|,$$

$$\|\phi_{i+1} - \phi_i\|\Bigg) < e_{tol}.$$

The value of e_{tol} is chosen as 10^{-8}. Further details of the solution methodology can be seen in our recently published work [44–47].

A numerical data comparison to validate our code is presented in Table 2. The results are correlated with those obtained by Rasool et al. [48]. The results of limiting cases for distinct values of Forchheimer parameter are consistent. Rasool et al. [48] used HAM and SOR to numerically solve and numerically interpret the problem, respectively. Our results are found to be in exceptional agreement with the existing ones. The validity of the code ensures the development of novel results of the concerned work.

4. Results and discussion

This section presents our analysis in graphical and tabular forms to explore the effects of various physical parameters involved in the present problem on velocity, temperature, and concentration. Assigning distinct values to the parameters may produce better results than specifying the particular values or domain dimensions (see [49,50]). Obviously, the certain applications
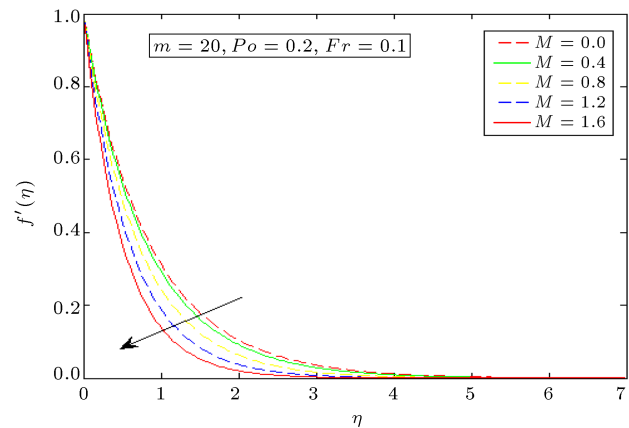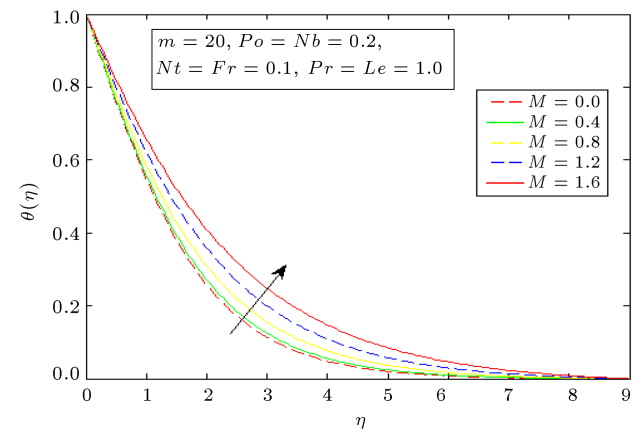

Figure 2. Effect of M on velocity.
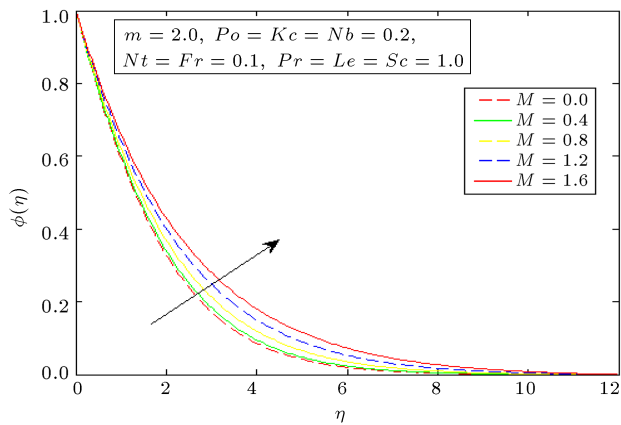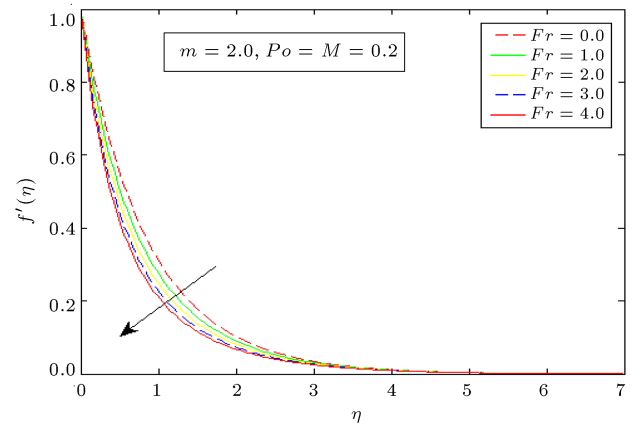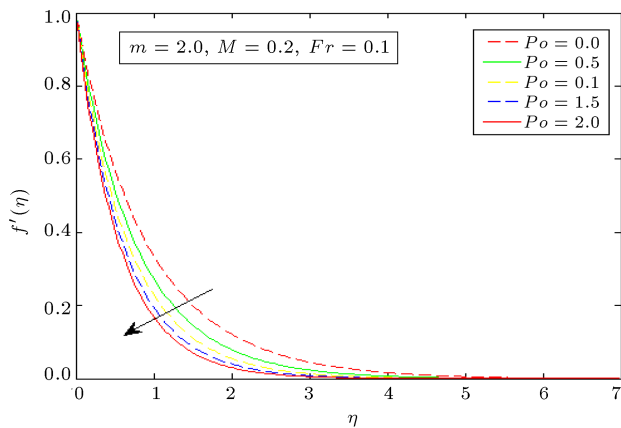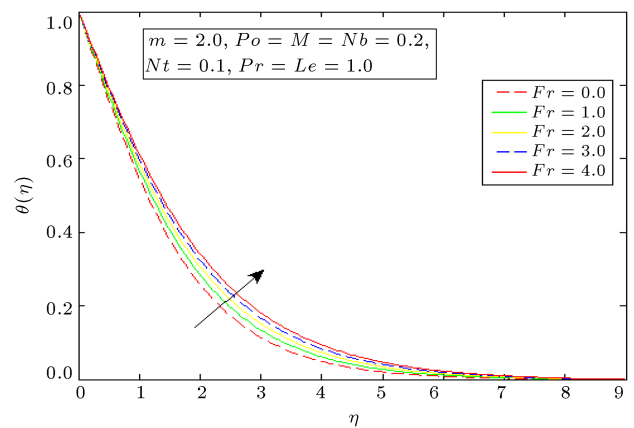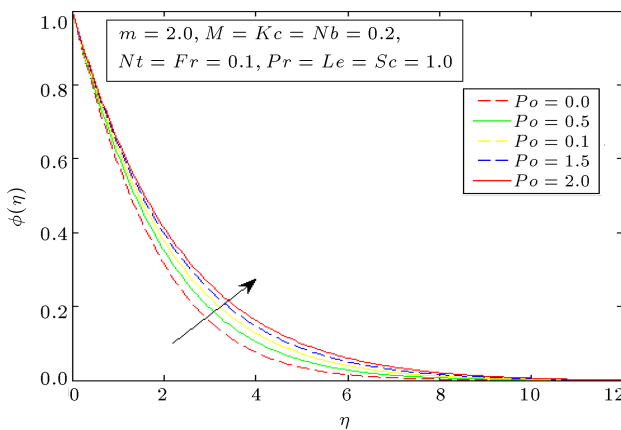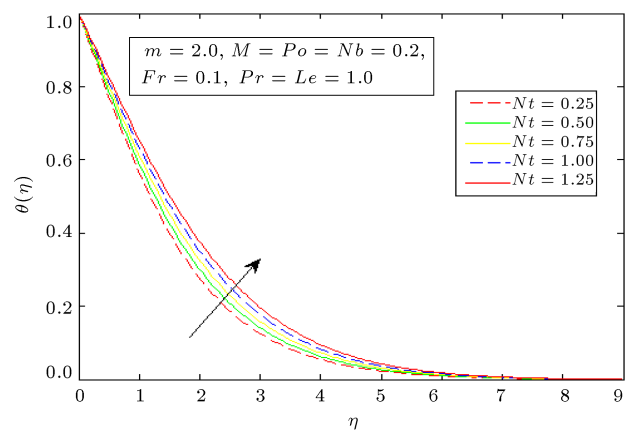

Figure 3. Effect of M on temperature.

of the problem may not require particular values; consequently, we need to specify the required values in such cases. In the problem under consideration, we have developed our results using the following ranges of parameters:

$$0 \leq M \leq 1.6, \quad 0 \leq P_0 \leq 2, \quad 0 \leq F_r \leq 4,$$

$$0.25 \leq N_t \leq 1.25, \quad 0.1 \leq S_c \leq 0.5,$$

$$0.50 \leq N_b \leq 2.5, \quad \text{and} \quad 0 \leq K_c \leq 2.5.$$

The impacts of an applied magnetic field are shown in Figures 2–4. A strong Lorentz force is induced due to the applied magnetic field, which causes a reduction in the flow velocity. Figures 5 and 6 illustrate the impact of the porosity factor on the non-dimensional velocity and concentration. The contribution of the Darcy parameter, i.e., porosity factor, raises the drag force on the surface of the sheet, which reduces the movement of the fluid. Due to the enhancement of the values of the porosity factor, velocity component and the thickness of the boundary layer are reduced. Moreover, the mass transfer is improved when close to the sheet for porosity. Figures 7 and 8 display the

Figure 4. Effect of M on concentration.

Figure 5. Effect of Po on velocity.

Figure 6. Effect of Po on concentration.

Figure 7. Effect of Fr on velocity.

Figure 8. Effect of Fr on temperature.

Figure 9. Effect of Nt on temperature.

effect of Forchheimer parameter on the temperature and velocity. The increase in Forchheimer number does not increase the velocity field and the resulting boundary layer is reduced, while temperature increases. It is worth mentioning that the effect of the local inertial force on the velocity and temperature profiles is more significant than that of the Darcy porosity factor.

The impact of thermophoretic parameter on the temperature distribution is shown in Figure 9. The temperature and the thickness of boundary layer are enhanced upon increasing values of thermophoretic parameter. In the case of vigorous thermophoretic force, the particles experience an increase in their dispersion because fluid travels from a hotter to cooler fluid region. Consequently, the existence of thermophoresis leads to increase in the temperature. Figure 10 designates
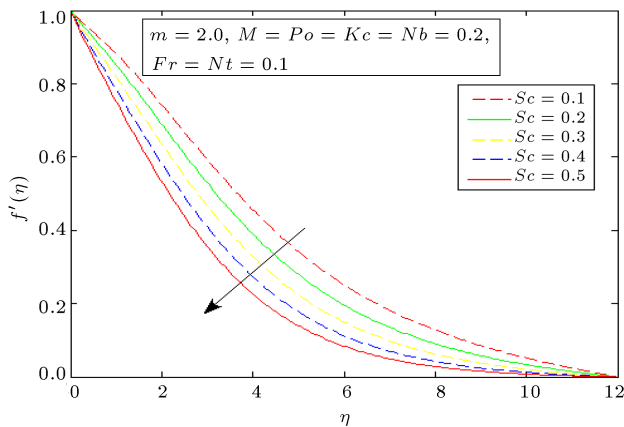
Figure 10. Effect of Sc on concentration.

Figure 11. Effect of Nb on concentration.

Figure 12. Effect of Kc on concentration.

Table 3. C_{f_x}, Nu_x, Sh_x for different M's.

M	C_{f_x}	Nu_x	Sh_x
0.0	1.483476	0.586614	0.577156
0.4	1.561806	0.572419	0.566494
0.8	1.775125	0.535526	0.540934
1.2	2.080611	0.487371	0.511922
1.6	2.442225	0.437533	0.486438

Table 4. C_{f_x}, Nu_x, Sh_x for different Fr's.

Fr	C_{f_x}	Nu_x	Sh_x
0.0	1.471687	0.586143	0.576632
1.0	1.764180	0.557552	0.556767
2.0	2.013861	0.534436	0.541521
3.0	2.234201	0.515020	0.529296
4.0	2.432876	0.498287	0.519192

Table 5. C_{f_x}, Nu_x, Sh_x for different Po's.

Po	C_{f_x}	Nu_x	Sh_x
0.0	1.400433	0.602035	0.589280
0.5	1.645219	0.557681	0.555918
1.0	1.856450	0.522161	0.532408
1.5	2.045040	0.492690	0.514901
2.0	2.216919	0.467688	0.501349

Table 6. Sh_x for different Kc's.

Kc	Sh_x
0.0	0.466143
0.5	0.706921
1.0	0.883532
1.5	1.028440
2.0	1.153811

the effect of Schmidt number on the concentration of nanoparticles. The Schmidt number describes the mass movement layer and hydrodynamic width layer. With an increment in the Schmidt number, the mass dispersion declines, which results in the reduction of the concentration. Figure 11 plots the concentration of nanoparticles to examine the variation of Brownian diffusion. An increment in the parameter of Brownian motion tends to reduce the concentration. Figure 12 elucidates the effect of chemical reaction factor on the dimensionless temperature. A catastrophic result was found which caused the reactant species to decay. Thus, the boundary layer for the associated chemical reaction was reduced.

The shear stresses as well as heat and mass transport rates for distinct values of the magnetic field are portrayed in Table 3. The values of skin friction seem to be increasing, whereas all values of Nu_x and Sh_x exhibit decreasing demeanor with the impact of M. Tables 4 and 5 reveal the impact of Forchheimer parameter Fr and porosity parameter Po on physical quantities like Sherwood number, skin friction, and Nusselt number for fixed values of M, Nb, Nt, Kc, Sc, and m. The effects of both Fr and Po are to elevate the surface drag (skin friction), but to devaluate the mass as well as heat transport rate on the surface of the sheet. The analysis of chemical reaction for mass transport rate is presented in Table 6. Different values of Kc sufficiently increase the rate of mass transfer.

5. Conclusions

Magnetohydrodynamic Darcy-Forchheimer nanofluid flow involving the chemical reaction over a nonlinearly stretching surface was explored in the present work. The governing equations were first transformed into ODEs and then, solved numerically by implementing Successive Over Relaxation (SOR) technique with MATLAB package. Significant conclusions may be listed as follows:

- Increase in values of Forchheimer, magnetic, and porosity parameters tends to reduce the magnitude of the velocity;

- Both the Nusselt and Sherwood numbers are devaluated with respect to the impact of porosity and Forchheimer parameter;

- The thermal boundary layer is enhanced for thermophoresis parameter and the concentration boundary layer is reduced for Brownian motion parameter;

- Concentration of nanoparticles is a decreasing function of Brownian motion and chemical reaction;

- The magnetic field parameter, porosity of medium, and local inertial force increase the skin friction coefficient.

Nomenclature

x, y	Space coordinates (m)
u, v	Velocity components (m.s^{-1})
ν	Kinematic viscosity of fluid (m^2.s^{-1})
μ	Dynamic viscosity of the fluid (Pa.s)
B	Strength of magnetic field (A.m^{-1})
m	Positive real no.
ρ_A	Density of fluid (kg.m^{-3})
K	Permeability (H.m^{-1})
C_b	Drag force coefficient (dimensionless)
L	Porosity factor
C_f	Skin friction/wall shear stress $C_f = \frac{T_w}{\rho U^2}$
Nb	Brownian diffusion parameter
Nu_x	Local Nusselt number
η	Dimensionless variable
θ	Dimensionless temperature
A	Thermal conductivity of base fluid (W.m^{-1} K^{-1})
T	Temperature (K)
T_w	Wall temperature (K)
T_∞	Ambient temperature (K)
$(\rho c)_{fl}$	Productive fluid heat capacity (J.m^{-3}.k^{-1})
$(\rho c)_{np}$	Productive nanoparticles heat capacity (J.m^{-3}.k^{-1})
Pr	Prandtl number
D_{Br}	Brownian diffusion
D_{th}	Thermophoresis effect
Fr	Forchheimer number
M	Magnetic number
N_t	Thermophoretic parameter
Nh_x	Local Sherwood number
f'	Dimensionless velocity
ϕ	Dimensionless concentration

References

1. Kandasamy, R., Hayat, T., and Obaidat, S. "Group theory trans-formation for Soret and Dufour effects on free convective heat and mass transfer with thermophoresis and chemical reaction over a porous stretching surface in the presence of heat source/sink", *Nucl. Eng. Des.*, **241**, pp. 2155–2161 (2011).

2. Gangadhar, K. and Bhaskar, N.R. "Chemically reacting MHD boundary layer flow of heat and mass transfer over a moving vertical plate in a porous medium with suction", *J. Appl. Mech.*, **6**, pp. 101–114 (2013).

3. Makinde, O.D., Khan, W.A., and Khan, Z.H. "Buoyancy effects on MHD stagnation point flow and heat transfer of a nanofluid past a convectivity heated stretching/shrinking sheet", *Int. J. Heat Mass Transf.*, **62**, pp. 526–533 (2013).

4. Turkyilmazoglu, M. "Latitudinally deforming rotating sphere", *Appl. Math. Model.*, **71**, pp. 1–11 (2019).

5. Choi, S.U. and Eastman, J.A. "Enhancing thermal conductivity of fluids with nanoparticles developments and applications of non-Newtonian flows", *D.A. Siginer and H.P. Wang* (New York ASME), **66**, pp. 99–105 (1995).

6. Masuda, H., Ebata, A., Teramae, K., et al. "Alteration of thermal conductivity and viscosity of liquid by dispersing ultra-fine particles", *Netsu. Bussei*, **7**, pp. 227–33 (1993).

7. Buongiorno, J. "Convective transport in nanofluids", *ASME Journal of Heat Transfer*, **128**, pp. 40–250 (2006).

8. Khan, W.A. and Pop, I. "Boundary-layer flow of a nanofluid past a stretching sheet", *Int. J. Heat Mass Transf.*, **53**, pp. 2477–2483 (2010).

9. Turkyilmazoglu, M. "Nanoliquid film flow due to a moving substrate and heat transfer", *Eur. Phys. J. Plus.*, **135**, p. 781 (2020).

10. Feizabad, K.M.H., Khayati, G.R., and Pouresterabadi, S. "Design and synthesis of carbon nanotubes for adsorption utilities: An approach to direct preparation by mechanical milling at room temperature", *Scientia Iranica*, **28**(3), pp. 1884–1895 (2021).

11. Jabeen, S., Hayat, T., and Alsaedi, A. "Entropy generation optimization and activation energy in flow of Walters-B nanomaterial", *Scientia Iranica*, **28**(3), pp. 1917–1925 (2021).

12. Hakeem, A.K.A., Indumathi, N., Ganga, B., et al. "Comparison of disparate solid volume fraction ratios of hybrid nanofluids flow over a permeable flat surface with aligned magnetic field and Marangoni convection", *Scientia Iranica*, **27**(6) pp. 3367–3380 (2020).

13. Jamshed, W., Devi, S.U., Goodarzi, M., et al. "Evaluating the unsteady Casson nanofluid over a stretching sheet with solar thermal radiation: An optimal case study", *Case Stud. Therm. Eng.* **26**, p. 101160 (2021).

14. Khan, A.U., Khan, S.I., Khan, U., et al. "Thermal transport investigation in AA7072 and AA7075 aluminum alloys nanomaterials based radiative nanofluids by considering the multiple physical flow conditions", *Sci Rep11*, **9837** (2021). https://doi.org/10.1038/s41598-021-87900-w

15. Gowda, R.J.P., Kumar, R.N., Jyothi, A.M., et al. "KKL correlation for simulation of nanofluid flow over a stretching sheet considering magnetic dipole and chemical reaction", *ZAMM*, **101**(11), Paper ID e202000372 (2021). https://doi.org/10.1002/zamm.202000372

16. Jamshed, W. and Nisar, K.S. "Computational single-phase comparative study of a Williamson nanofluid in a parabolic trough solar collector via the Keller box method", *Int. J. Energy Res.* **45**(7), pp. 10696–10718 (2021).

17. Jamshed, W., Akgül, E.K., and Nisar, K.S. "Keller box study for inclined magnetically driven Cassonnano fluid over a stretching sheet: single phase model", *Phys. Scr. 96 065201*, **96**(6), Paper ID 065201 (2021)

18. Jamshed, W., Devi, S.U., and Nisar, K.S. "Single phase based study of Ag-Cu/EO Williamson hybrid nanofluid flow over a stretching surface with shape factor", *Phys. Scr. 96 065202*, **96**(6), Paper ID 065202 (2021).

19. Sharma, P.R. and Singh, G. "Effects of variable thermal conductivity and heat source/sink on MHD flow near a stagnation point on a linearly stretching sheet", *J. Appl. Fluid. Mech.*, **2**, pp. 13–21 (2019).

20. Aziz, A. and Khan, W.A. "Classical and minimum entropy generation analyses for steady state conduction with temperature dependent thermal conductivity and asymmetric thermal boundary conditions, regular and functionally graded materials", *Energy J.*, **36**, pp. 6195–6207 (2011).

21. Pal, D. and Chatterjee, S. "Soret and Dufour effects on MHD convective heat and mass transfer of power law fluid over an inclined plate with variable thermal conductivity in a porous medium", *Appl. Math. Comput.*, **219**, pp. 7556–7574 (2013).

22. Hakeem, A.K.A., Ganesh, N.V., and Ganga, B. "Magnetic field effect on second order slip flow of nanofluid over a stretching/shrinking sheet with thermal radiation effect", *J. Magn. Magn. Mater.*, **381**, pp. 243–257 (2015).

23. Turkyilmazoglu, M. "Multiple analytic solutions of heat and mass transfer of Magneto hydrodynamic slip flow for two types of viscoelastic fluids over a stretching surface", *Hacettepe Üniversitesi Akademik Veri Yönetim Sistemi*, **134**, p. 7 (2012). DOI: 10.1115/1.4006165

24. Darcy, H., *Les fontaines publiques de la ville de Dijon*, Paris: Victor Dalmont (1856).

25. Ram, G. and Verma, R.S. "Unsteady flow through MHD porous media Indian", *I. Appl. Math.*, **8**, pp. 637–647 (1977).

26. Zhang, R., Ning, Z., Yang, F., et al. "Laboratory study of the porosity permeability relationships of shale and sandstone under effective stress", *Int. J. Rock Mech. Min. Sc.*, **81**, pp. 19–27 (2016).

27. Sheikholeslami, M., Jafaryar, M., Said, Z., et al. "Modification for helical turbulator to augment heat transfer behavior of nanomaterial via numerical approach", *Appl. Therm. Eng.*, **182**, p. 115935 (2021).

28. Hayat, T., Rafique, K., Muhammad, T., et al. "Carbon nanotubes significance in Darcy-Forchheimer flow", *Results in Physics.*, **8**, pp. 26–33 (2018).

29. Turkyilmazoglu, M. "Stretching/shrinking longitudinal fins of rectangular profile and heat transfer", *Energy Convers. Manag.*, **91**, pp. 199–203 (2015).

30. Turkyilmazoglu, M. "On the transparent effects of Buongiorno nanofluid model on heat and mass transfer", *Eur. Phys. J. Plus.*, **136**, p. 376 (2021).

31. Ali, K., Ahmad, S., Nisar, K.S., et al. "Simulation analysis of MHD hybrid CuAl2O3/H2O nanofluid flow with heat generation through a porous media", *Int. J. Energy Res.*, pp. 1–15 (2021). https://doi.org/10.1002/er.7016

32. Sheikholeslami, M., Farshad, S.A., Ebrahimpour, Z., et al. "Recent progress on flat plate solar collectors and photovoltaic systems in the presence of nanofluid: A review", *J. Clean. Prod.*, **293**, p. 126119 (2021).

33. Caucao, S., Gatica, G.N., and Sandoval, F. "A fully-mixed finite element method for the coupling of the Navier-Stokes and Darcy-Forchheimer equation", *Numer. Methods Partial Differ. Equ.*, **37**(3), pp. 2550–2587 (2021). https://doi.org/10.1002/num.22745

34. Ganesh, N.V., Hakeem, A.K.A., and Ganga, B. "Darcy-Forchheimer flow of hydromagnetic nanofluid over a stretching/shrinking sheet in a thermally stratified porous medium with second order slip, viscous and Ohmic dissipations effects", *Ain Shams Eng. J.*, **9**, pp. 939–951 (2018).

35. Ullah, M.Z., Capizzano, S.S., and Baleanu, S.D. "A numerical simulation for Darcy-Forchheimer flow of nanofluid by a rotating disk with partial slip effect", *Front. Phys.*, **7**(N/A), Paper ID 219 (2020). https://doi.org/10.3389/fphy.2019.00219

36. Khan, A., Shah, Z., Islam, S., et al. "Darcy-Forchheimer flow of micropolar nanofluid between two plates in the rotating frame with non-uniform heat generation/absorption", *Adv. Mech. Eng.*, **10**(10), pp. 1–16 (2018).

37. Du, G., Li, Q., and Zhang, Y. "A two-grid method with back tracking for the mixed Navier-Stokes/ Darcy model", *Numer. Methods Partial Differ. Equ.*, **36**, pp. 1601–1610 (2020).

38. Khan, U., Zaib, A., Khan, I., et al."Insights into the stability of mixed convective darcy-forchheimer flows of cross liquids from a vertical plate with consideration of the significant impact of velocity and thermal slip conditions", *Mathematics.*, **8**(1), p. 31 (2020). https://doi.org/10.3390/math8010031

39. Lund, L.A., Ling, D., Ching, C., et al. "Triple local similarity solutions of darcy-forchheimer magnetohydrodynamic (MHD) flow of micropolar nanofluid over an exponential shrinking surface stability analysis", *Coatings.*, **9**(8) p. 527 (2019). https://doi.org/10.3390/coatings9080527

40. Rasool, G., Shafiq, A., Khan, A., et al. "Entropy generation and consequences of MHD in darcy-forchheimer nanofluid flow bounded by non-linearly stretching surface", *Symmetry*, **12**(4), p. 652 (2020). https://doi.org/10.3390/sym12040652

41. Lund, L.A., Omar, Z., Khan, U., et al. "Stability analysis and dual solutions of micropolar nanofluid over the inclined stretching/shrinking surface with convective boundary condition", *Symmetry*, **12**(1), p. 74 (2020). https://doi.org/ 10.3390 /sym12010074

42. Kala, B.S., Singh, M., and Kumar, A. "Steady MHD free convective flow and heat transfer over nonlinearly stretching sheet embedded in an extended Darcy-Forchheimer porous medium with viscous dissipation", *J. Global. Res. Math. Arc.*, **2**, pp. 1–15 (2014).

43. Geraki, C.F. and Wheatley, P.O., *Applied Numerical Analysis*, Addison-Wesley Publishing Company, Massachusetis (2004).

44. Ahmad, S., Ali, K., Rizwan, M., et al. "Heat and mass transfer attributes of copper aluminum oxide hybrid nanoparticles flow through a porous medium", *Case Stud. Therm. Eng.*, **25**, p. 100932 (2021). https://doi.org/10.1016/j.csite.2021.100932

45. Ahmad, S., Ali, K., and Ashraf, M. "MHD flow of CU-AL2O3/water hybrid nanofluid through a porous media", *Journal of Porous Media.*, **24**, pp. 61–73 (2021).

46. Ahmad S., Ali, K., Ashraf, M. et al. "Numerical study of lorentz force interaction with micro structure in channel flow", *Energies*, **14**(14), p. 4286 (2021). https://doi. org /10.3390/en14144286

47. Ahmad, S., Ashraf, M., and Ali, K. "Numerical simulation of viscous dissipation in a micropolar fluid flow through a porous medium", *J. Appl. Mech. Tech. Phy.*, **60**(6), pp. 996–1004 (2019).

48. Rasool, G., Shafiq, A., Kalique, C.M., et al. "MHD darcy-forchheimer nanofluid flow over a nonlinear stretching sheet", *Phys. Scr.*, **94**(10), pp. 1–24 (2019).

49. Ahmad, S., Ashraf, M., and Ali, K. "Simulation of thermal radiation in a micropolar fluid flow through a porous medium between channel walls", *J. Therm. Anal. Calorim.*, **144**, pp. 941–953 (2021)

50. Ahmad, S., Ashraf, M., and Ali, K. "Nanofluid flow comprising gyrotactic micro organisms through a porous medium", *J. Appl. Fluid. Mech.*, **144**(3), pp. 1539–1549 (2020).

Biographies

Muhammad Imran Shahid is a PhD scholar under the supervision of Dr. Ashraf in the Centre for Advanced Studies in Pure and Applied Mathematics, Bahauddin Zakariya University, Multan, Pakistan. He is an Assistant Professor at the Department of Mathematics, Government College of Science, Multan 60000, Pakistan.

Sohail Ahmad is a PhD scholar under the supervision of Professor Ashraf at the Centre for Advanced Studies in Pure and Applied Mathematics, Bahauddin Zakariya University, Multan, Pakistan. His doctoral research investigates the heat and mass transfer, computational fluid dynamics, thermal analysis, advances in nanofluids, numerical study of flows through porous media, and magnetohydrodynamics. He takes a multidisciplinary approach that encompasses the fields of applied mathematics, bio-mechanics, fluid mechanics, mathematical physics, and mechanics. He is a potential reviewer of several international journals. Recently, he has authored twelve publications.

Muhammad Ashraf is working as a Professor at the Centre for Advanced Studies in Pure and Applied Mathematics, Bahauddin Zakariya University, Multan, Pakistan. He has a teaching experience of more than 25 years. He employed various numerical methods such as Successive over Relaxation Method, Quasi-linearization Method, Differential Transform Method, and successive under Relaxation method in his publications. He has supervised many MPhil and PhD students and has numerous publications on his account in impact-factor-bearing international journals. His research interests include multiphase fluid-particle dynamics, nanofluids flow modeling, transport in porous media, heat and mass transfer, magnetohydrodynamics, numerical analysis, heat and fluids, computational fluid dynamics, modeling of fluid flow problems, nonlinear science, and ferrohydrodynamic, electrohydrodynamic, and numerical simulation of mathematical models.